Forty-Sixth Annual Allerton Conference
Allerton House, UIUC, Illinois, USA
September 23-26, 2008



# Range-Based Geolocation in Fading Environments

Brian M. Sadler
Army Research Laboratory
AMSRD-ARL-CI-NT
Adelphi, MD 20783
bsadler@arl.army.mil

Ning Liu, Zhengyuan Xu
Dept. of Electrical Engineering
University of California
Riverside, CA 92521
dxu@ee.ucr.edu

Richard Kozick
Dept. of Electrical Engineering
Bucknell University
Lewisburg, PA 17837
kozick@bucknell.edu

***Abstract*— We consider source geolocation based on range estimates from sensors with known coordinates. In a fading propagation environment, where a line-of-sight (LOS) path may be weak or essentially nonexistent, range estimates may have positive biases. We study this problem by considering a weighted least squares (WLS) location estimator, based on noisy range estimates, each of which is contaminated by additive Gaussian noise and possibly a positive bias. We derive the mean and mean-square error (MSE) of the WLS estimator, showing that in general the estimator produces biased estimates. The error expressions are developed via first-order perturbation analysis. They provide a means to study achievable localization performance, as a function of the measurement bias and variance, as well as the sensor network geometry.**

## I. Introduction

Solutions to the geolocation problem in a sensor network can be categorized in various ways, such as methods that utilize range measurements and those that do not [1]. For example, range-free techniques can rely on angle-of-arrival measurements, or node connectivity [2], [3]. Range-based techniques typically use time-of-arrival [4], [5] or received signal strength [6], to estimate the distance of neighboring nodes. Different measurement modalities can be combined to improve location estimation (e.g., see [7]).

In this paper we consider source geolocation based on multiple range estimates from sensors with known location. In a fading propagation environment, where a line-of-sight (LOS) path may be weak or essentially nonexistent, range estimates may have a positive bias. We study this problem by considering a weighted least squares (WLS) location estimator, based on noisy range estimates contaminated by additive Gaussian noise and possibly a bias, where the bias may be different for each sensor. We derive the mean, and mean-square error (MSE), of the WLS estimator, showing that in general it produces biased estimates. The error expressions are developed via first-order perturbation analysis. They provide a means to study achievable localization performance, as a function of the measurement bias and variance, as well as the sensor network geometry.

In related recent work, Weiss and Picard have studied geolocation with biased range measurements, where the bias is identical for all sensors [8]. Jourdan and coauthors have developed a localization bound with biased measurements in an ultra-wideband environment, where the bias statistics were obtained experimentally for an indoor scenario [9].

Range measurement is often accomplished based on time delay estimation (TDE). We have developed Ziv-Zakai bounds (ZZBs) on TDE for wideband wireless fading channels [10], [11], [12]. These results can be combined with the analysis in this paper to study localization error based on TDE measurements.

## II. System Model

Consider a range-based localization problem employing $K$ sensors at known locations $(x_i,\ y_i)$, $i = 1, \cdots, K$. The source is located at unknown location $(x_s,\ y_s)$. The range from the source to the $i$-th sensor is

$$r_i = \sqrt{a_i^2 + b_i^2}, \tag{1}$$

or equivalently

$$r_i^2 = a_i^2 + b_i^2, \tag{2}$$

where

$$a_i = x_s - x_i, \quad b_i = y_s - y_i. \tag{3}$$

We consider estimation of $(x_s,\ y_s)$ based on estimates of $r_i$, $i = 1, \cdots, K$, in a noisy fading channel. We model the range measurement at the $i$-th sensor by

$$m_i = r_i + n_i, \quad n_i = \mu_i + v_i, \tag{4}$$

where $\mu_i \geq 0$ is a bias assumed to be independent of the source location, and $v_i$ is assumed to be white noise with zero mean, standard deviation $\sigma$ and independent across sensors. We assume that any range bias is strictly positive, due to multipath propagation when the line-of-sight path is weak or essentially non-existent. In this paper we treat the bias as an unknown deterministic constant, that varies from sensor to sensor, and may be zero for a subset of sensors. Our analysis can be easily generalized to accommodate correlated noise.

## III. Range Measurements with Deterministic Unknown Biases

### A. Weighted Least Squares Estimation

Consider weighted least squares (WLS) estimation of the source location, given by

$$\min_{(x_s, y_s)} \sum_{i=1}^{K} (m_i - r_i)^2 w_i, \tag{5}$$

This work was supported in part by the Army Research Laboratory CTA on Communications and Networks under grant DAAD19-01-2-0011.

where $w_i$ is a weight that can be chosen as desired, for example letting $w_i = \sigma_i^{-2}$.

The solution to the optimization problem (5) can be obtained by differentiating with respect to both $x_s$ and $y_s$ and equating with zero. Note that only $r_i$ is a function of the unknown location. From (1) and (3) we have

$$\frac{dr_i}{dx_s} = \frac{a_i}{r_i}, \quad \frac{dr_i}{dy_s} = \frac{b_i}{r_i}. \tag{6}$$

Accordingly, the optimal solution satisfies the following two equations

$$\sum_{i=1}^{K}(m_i - r_i)\frac{w_i a_i}{r_i} = 0, \tag{7}$$

$$\sum_{i=1}^{K}(m_i - r_i)\frac{w_i b_i}{r_i} = 0. \tag{8}$$

These are highly nonlinear in $x_s$ and $y_s$ due to (1) and (3), but can be solved numerically.

### *B. First order geolocation error analysis*

To study the estimation error from the estimator (5), we next carry out a perturbation analysis around the optimal solution $(x_s, y_s)$, e.g., see [13]. Let $\delta m_i = n_i$ denote a small measurement error that includes the measurement bias and noise. The error $\delta m_i$ causes an estimation error $\delta x_s$, $\delta y_s$, and associated errors $\delta r_i$ in $r_i$, $\delta a_i$ in $a_i$, and $\delta b_i$ in $b_i$, with $x_i$ and $y_i$ assumed known. Sensor position errors are omitted here but can be incorporated easily.

Note that the perturbed quantities still satisfy (7) and (8). Under the small error assumption, perturbation analysis is equivalent to differentiation, i.e., replacing the total differential operator $d$ by the error operator $\delta$ at the true solution point. In order to relate $\delta x_s$ and $\delta y_s$ to $\delta m_i$, we first re-express $\delta r_i$, $\delta a_i$ and $\delta b_i$. According to (1) and (3), and applying the total differential theorem, the first-order error terms are related by

$$\delta a_i = \delta x_s, \quad \delta b_i = \delta y_s. \tag{9}$$

$$\delta r_i \approx \frac{a_i}{r_i}\delta a_i + \frac{b_i}{r_i}\delta b_i = \frac{a_i}{r_i}\delta x_s + \frac{b_i}{r_i}\delta y_s. \tag{10}$$

Second-order perturbation analysis can be obtained via further differentiation of (10), with second-order perturbation $\delta^2 r_i$. This results in an error analysis that is valid over a broader range of noise levels; we defer this to future work.

Next, we relate $\delta x_s$ and $\delta y_s$ to $\delta m_i$ from equations (7) and (8), yielding two equations for $\delta x_s$ and $\delta y_s$. Beginning with (7), term-by-term differentiation yields

$$\sum_{i=1}^{K} w_i[\delta(\frac{m_i a_i}{r_i}) - \delta a_i] = 0. \tag{11}$$

The inside term can be expanded as

$$\begin{aligned}\delta(\frac{m_i a_i}{r_i}) &\approx \frac{\delta(m_i a_i) r_i - m_i a_i \delta r_i}{r_i^2} \\ &\approx \frac{\delta m_i a_i + m_i \delta a_i}{r_i} - \frac{m_i a_i \delta r_i}{r_i^2}.\end{aligned} \tag{12}$$

Substituting (9) and (10) and noting $r_i^2 - a_i^2 = b_i^2$, the above becomes

$$\delta(\frac{m_i a_i}{r_i}) \approx \frac{a_i}{r_i}\delta m_i + \frac{m_i b_i^2}{r_i^3}\delta x_s - \frac{a_i b_i m_i}{r_i^3}\delta y_s. \tag{13}$$

Substituting (9) and (13) into (11) and combining corresponding terms, we obtain

$$\sum_{i=1}^{K} w_i[(1 - \frac{m_i b_i^2}{r_i^3})\delta x_s + \frac{m_i a_i b_i}{r_i^3}\delta y_s] \approx \sum_{i=1}^{K}\frac{w_i a_i}{r_i}\delta m_i. \tag{14}$$

In our error analysis, $m_i$ represents the measurement in the absence of error $n_i$, and $\delta m_i$ represents the error $n_i$. Replacing $m_i$ by $r_i$ and $\delta m_i$ by $n_i$, the above becomes

$$c_{11}\delta x_s + c_{12}\delta y_s \approx \boldsymbol{d}_1^T \boldsymbol{n}, \tag{15}$$

where

$$c_{11} = \sum_{i=1}^{K}\frac{w_i a_i^2}{r_i^2}, \quad c_{12} = \sum_{i=1}^{K}\frac{w_i a_i b_i}{r_i^2}, \tag{16}$$

$$\boldsymbol{d}_1^T = [\frac{w_1 a_1}{r_1}, \cdots, \frac{w_K a_K}{r_K}], \quad \boldsymbol{n}^T = [n_1, \cdots, n_K]. \tag{17}$$

This is the first equation to relate location errors to the measurement noise.

Starting from (8) and following a similar procedure, we obtain the second error equation

$$c_{21}\delta x_s + c_{22}\delta y_s \approx \boldsymbol{d}_2^T \boldsymbol{n}, \tag{18}$$

where

$$c_{21} = c_{12}, \quad c_{22} = \sum_{i=1}^{K}\frac{w_i b_i^2}{r_i^2},$$

$$\boldsymbol{d}_2^T = [\frac{w_1 b_1}{r_1}, \cdots, \frac{w_K b_K}{r_K}].$$

We can combine (15) and (18), to obtain

$$\boldsymbol{C}\delta\boldsymbol{p} \approx \boldsymbol{D}\boldsymbol{n}, \tag{19}$$

where

$$\boldsymbol{C} = \begin{bmatrix} c_{11} & c_{12} \\ c_{21} & c_{22} \end{bmatrix}, \quad \delta\boldsymbol{p} = \begin{bmatrix} \delta x_s \\ \delta y_s \end{bmatrix}, \quad \boldsymbol{D} = \begin{bmatrix} \boldsymbol{d}_1^T \\ \boldsymbol{d}_2^T \end{bmatrix}. \tag{20}$$

So the first order estimation error vector for source location is

$$\delta\boldsymbol{p} \approx \boldsymbol{C}^{-1}\boldsymbol{D}\boldsymbol{n} = \boldsymbol{G}\boldsymbol{n}, \tag{21}$$

where

$$\boldsymbol{G} = \boldsymbol{C}^{-1}\boldsymbol{D}. \tag{22}$$

Eq. (21) is the desired relation of location perturbation error $\delta\boldsymbol{p}$ with measurement noise and system parameters. The MSE of the estimator is

$$\mathrm{MSE}_{\mathrm{WLS}} = E\{|\delta\boldsymbol{p}|^2\} \approx tr\{\boldsymbol{G}\boldsymbol{\Phi}_n\boldsymbol{G}^T\}, \tag{23}$$

where $\boldsymbol{\Phi}_n$ is the correlation matrix of $\boldsymbol{n}$. Stacking the range bias from different sensor measurements in the vector $\boldsymbol{\mu}$, then the correlation matrix is related to bias and noise variance by

$$\boldsymbol{\Phi}_n = E(\boldsymbol{n}\boldsymbol{n}^T) = \boldsymbol{\mu}\boldsymbol{\mu}^T + \mathrm{diag}\{\sigma_1^2, \cdots, \sigma_K^2\}. \tag{24}$$

The resulting bias in the location estimate is given by $E\{\delta \boldsymbol{p}\}$

$$E\{\delta \boldsymbol{p}\} \approx \boldsymbol{G}\boldsymbol{\mu}. \quad (25)$$

Thus the WLS estimator will be biased in general if $\boldsymbol{\mu} \neq \mathbf{0}$. However, it is possible for the estimator bias to become zero while $\boldsymbol{\mu} \neq \mathbf{0}$ for some special cases.

## IV. Error analysis in polar coordinates

A polar coordinate system with its origin at the unknown source location can significantly simplify the expressions of the elements of $\boldsymbol{C}$ and $\boldsymbol{D}$. In this polar coordinate system, the $i$-th sensor is located at $(r_i, \theta_i)$. For convenience, we retain the original Cartesian coordinate system to express the source location and its estimation error. This dual-system approach will be clear in context. Applying $a_i = r_i \cos\theta_i$ and $b_i = r_i \sin\theta_i$, we obtain

$$c_{11} = \sum_{i=1}^{K} w_i \cos^2\theta_i = \sum_{i=1}^{K} \frac{1}{2} w_i + \sum_{i=1}^{K} \frac{1}{2} w_i \cos 2\theta_i, \quad (26)$$

$$c_{22} = \sum_{i=1}^{K} w_i \sin^2\theta_i = \sum_{i=1}^{K} \frac{1}{2} w_i - \sum_{i=1}^{K} \frac{1}{2} w_i \cos 2\theta_i, \quad (27)$$

$$c_{12} = c_{21} = \sum_{i=1}^{K} w_i \sin\theta_i \cos\theta_i = \sum_{i=1}^{K} \frac{1}{2} w_i \sin 2\theta_i, \quad (28)$$

$$\boldsymbol{D} = \begin{bmatrix} w_1 \cos\theta_1, \cdots, w_K \cos\theta_K \\ w_1 \sin\theta_1, \cdots, w_K \sin\theta_K \end{bmatrix}. \quad (29)$$

Next, we apply these expressions to study a localization example with a circular sensor array and the source at the origin.

### A. Circularly uniform array example

Consider an example where the sensors are uniformly and circularly placed around the source, so that $\theta_i = 2\pi(i-1)/K$. This includes linear, triangular and square sensor configurations, corresponding to $K = 2, 3, 4$, respectively. For simplicity, assume a common bias so that all elements in $\boldsymbol{\mu}$ are equal, i.e., $\boldsymbol{\mu} = \mu \mathbf{1}$ for $\mu \neq 0$. Let $w_i = w = \sigma^{-2}$ for all sensors. Under these assumptions, matrix $\boldsymbol{C}$ and vector $\boldsymbol{D}\boldsymbol{u}$ in (25) can be simplified based on the trigonometric identities

$$\cos x = \frac{1}{2}(e^{jx} + e^{-jx}), \quad \sin x = \frac{1}{2j}(e^{jx} - e^{-jx}), \quad (30)$$

where $j = \sqrt{-1}$, and geometric series

$$\begin{aligned} \sum_{k=1}^{K} e^{j(k-1)x} &= \frac{e^{jKx} - 1}{e^{jx} - 1} = \frac{e^{jKx/2}(e^{jKx/2} - e^{-jKx/2})}{e^{jx/2}(e^{jx/2} - e^{-jx/2})} \\ &= \frac{\sin\frac{Kx}{2}}{\sin\frac{x}{2}} e^{j\frac{K-1}{2}x}. \end{aligned} \quad (31)$$

Using (30) and (31), we have

$$\begin{aligned} \sum_{k=1}^{K} \cos(k-1)x &= \frac{1}{2}\Big[\sum_{k=1}^{K} e^{j(k-1)x} + \sum_{k=1}^{K} e^{-j(k-1)x}\Big] \\ &= \frac{\sin\frac{Kx}{2}\cos\frac{K-1}{2}x}{\sin\frac{x}{2}}, \end{aligned} \quad (32)$$

$$\begin{aligned} \sum_{k=1}^{K} \sin(k-1)x &= \frac{1}{2j}\Big[\sum_{k=1}^{K} e^{j(k-1)x} - \sum_{k=1}^{K} e^{-j(k-1)x}\Big] \\ &= \frac{\sin\frac{Kx}{2}\sin\frac{K-1}{2}x}{\sin\frac{x}{2}}. \end{aligned} \quad (33)$$

Substituting these results in (26), (27), (28), we obtain

$$c_{11} = c_{22} = \frac{1}{2} wK, \quad c_{12} = c_{21} = 0, \quad (34)$$

so that $\boldsymbol{C} = \frac{wK}{2}\boldsymbol{I}$. Similarly, we can find

$$\boldsymbol{d}_1^T \boldsymbol{\mu} = 0, \quad \boldsymbol{d}_2^T \boldsymbol{\mu} = 0.$$

Thus $\boldsymbol{D}\boldsymbol{\mu} = \mathbf{0}$, and applying this to (25) we find that $E\{\delta \boldsymbol{p}\} = \mathbf{0}$. Therefore, for this special geometry and with common measurement bias, the WLS estimation has no bias (up to the first order error). This is intuitively pleasing, and hints that spatially diverse sensor placement can reduce estimation bias.

The MSE (23) can also be simplified. For this special case $\boldsymbol{D}\boldsymbol{\mu} = \mathbf{0}$ and $\mathrm{diag}\{\sigma_1^2, \cdots, \sigma_K^2\} = \sigma^2 \boldsymbol{I}$. It can be easily verified that $\boldsymbol{D}\boldsymbol{D}^T = w\boldsymbol{C}$. Then (23) becomes

$$\mathrm{MSE}_{\mathrm{WLS}} \approx \sigma^2 tr\{\boldsymbol{C}^{-1}\boldsymbol{D}\boldsymbol{D}^T\boldsymbol{C}^{-1}\} = \frac{4\sigma^2}{K}. \quad (35)$$

The expression is consistent with the Cramér-Rao bound (CRB) of eq. (28) developed in [8] for the case of a common bias for all sensors. It is interesting that without any knowledge of the measurement bias, for this example, the WLS MSE approaches the CRB at high SNRs (i.e., under the small error assumption).

## V. Bias, variance, and Estimation Performance

Our analytical results on the location estimation bias and MSE relate WLS performance to measurement bias, noise variance, sensor locations, and LS weights. In this section we consider adjusting the weights and sensor locations to minimize localization error.

From (25), a general condition for WLS to produce unbiased location estimates is $\boldsymbol{G}\boldsymbol{\mu} = \mathbf{0}$, so that vector $\boldsymbol{\mu}$ is in the nullspace of $\boldsymbol{G}$. This can be achieved with $\boldsymbol{D}\boldsymbol{\mu} = \mathbf{0}$, i.e., when

$$\sum_{i=1}^{K} w_i \mu_i \cos\theta_i = 0, \quad \sum_{i=1}^{K} w_i \mu_i \sin\theta_i = 0. \quad (36)$$

This sufficient condition suggests a possible method for sensor placement and weight selection that results in a small location estimation bias.

To gain some insight on bias reduction, let $\mu_i = \mu$ and $w_i = w$. The squared norm of $\boldsymbol{D}\boldsymbol{\mu}$ can now be expressed as

$$\begin{aligned} |\boldsymbol{D}\boldsymbol{\mu}|^2 &= \mu^2 w^2 [(\sum_{i=1}^{K} \cos\theta_i)^2 + (\sum_{i=1}^{K} \sin\theta_i)^2] \\ &= 2\mu^2 w^2 \sum_{i_1, i_2 = 1}^{K} \cos(\theta_{i_1} - \theta_{i_2}). \\ &= 2\mu^2 w^2 [1 + \sum_{i_1 \neq i_2 = 1}^{K} \cos(\theta_{i_1} - \theta_{i_2})]. \end{aligned} \quad (37)$$

This quantity depends on the measurement bias $\mu$, and all possible sensor placement angle differences. Consider an extreme sensor configuration where all the sensors are located in a cluster at angle zero with respect to the source; then $|\boldsymbol{D\mu}|^2$ reaches its maximum value of $2K\mu^2w^2$ since all $\theta_i$ are equal. This worst case leads to a large estimation bias and consequently an increased MSE. Now suppose half of the sensors are located at angle zero, and the other half at angle 180 degrees. Then, the angle differences are either zero or 180 degrees with equal number of each. Consequently, $|\boldsymbol{D\mu}|^2$ reaches its minimum value of zero, and WLS is unbiased. This is also similar to the circular array case discussed in section IV-A. For arbitrary sensor configurations, $|\boldsymbol{D\mu}|^2$ takes a value between zero and its maximum. For example, if half the sensors are at angle zero and half at 90 degrees, then $|\boldsymbol{D\mu}|^2$ takes the medium value $K\mu^2w^2$. These examples indicate that sensor location angle diversity helps to reduce the impact of bias.

The LS weight can be employed to attempt to reduce the location error. Intuitively, according to (36), the weight for a particular sensor should be chosen to be smaller when the measurement bias is larger, although tuning the weight in this way requires additional information about the bias. It is also of interest to consider the bias-variance tradeoff. The MSE, given by (23), can also be minimized with respect to sensor locations and weights. In the next section we present some numerical results on the impact of bias and sensor placement.

## VI. Numerical examples

We compare WLS simulation performance and our error analysis. All results are based on averages over $10^4$ independent realizations. We adopt the following root mean-square-error (RMSE) and estimation bias for the source location as performance metrics [13]

$$\text{RMSE} = \sqrt{E\{(\delta x_s)^2\} + E\{(\delta y_s)^2\}},$$
$$\text{Bias} = \sqrt{(E\{\delta x_s\})^2 + (E\{\delta y_s\})^2},$$

and examine effects of different parameters on estimator performance, in particular measurement bias $\boldsymbol{\mu}$ and additive Gaussian noise standard deviation $\sigma$. For the simulations, the expectations in the RMSE and bias are replaced with sample averages. The WLS weights are set to $w_i = w = 1/\sigma^2$ in all experiments.

We consider $K = 10$ sensors either uniformly or non-uniformly distributed on a circle with normalized radius of one distance unit (DU), centered at the unknown source location. For the non-uniform configurations, the sensor location angles are randomly generated once in $[0, 2\pi)$ and fixed for the duration of the experiment. Note that the errors are expressed relative to the source range of 1 DU. Thus, for example, $\sigma = 0.1$ corresponds to Gaussian error with a standard deviation of $10\%$ of the true range (a large range error). Similarly, for example, a bias of $0.1$ DU is a significant range error.

Figure 1 depicts the RMSE of the WLS estimator against Gaussian noise standard deviation $\sigma$ for (a) uniform circular placement, and (b) non-uniform circular placement. For all sensors, the unknown bias is fixed to be either zero or $0.1$ DU, and the noise standard deviation is $\sigma$. The analytical results (dashed lines) are close to the simulation results (solid lines) for a range of $\sigma$, showing the range over which the first-order error analysis gives good prediction. As expected, the theory-simulation gap increases as $\sigma$ becomes large relative to the source range. The RMSE levels are comparable for the two different geometries at large $\sigma$, showing relative insensitivity to some randomization of the sensor placement for this example. The RMSE is linear with $\sigma$ for small $\sigma$, then increases more slowly for large $\sigma$.

Figure 2 is the same setup as Figure 1, but now $\sigma$ is restricted to a more reasonable error size ($\leq 0.2$ DU). The addition of measurement bias has a relatively small effect on the RMSE, and the bias effect is more predominant in the non-uniform array case, as expected from the error analysis for the uniform array. In particular, the RMSE with a non-uniform array shows a small error floor of less than $0.1$ DU even for a very small $\sigma$ due to the measurement bias, while this error floor does not occur in the uniform array case. At low SNR (large $\sigma$), the effect of the measurement bias is swamped by the noise, and addition of bias to the range measurement appears to have little additional effect on the RMSE.

Figure 3 shows WLS estimator bias versus $\sigma$ for the cases described above. The WLS location bias with a uniform array is very small, whether the measurement bias is zero or non-zero, as analytically predicted. With a non-uniform array, the estimation bias becomes nonzero for the displayed case of measurement bias equal to $0.1$ DU. However, the resulting estimation bias is less than $0.07$ DU. While small, this results in the RMSE error floor in Fig. 2(b) as $\sigma$ approaches zero.

Figure 4 depicts the impact of increasing bias on location estimate RMSE and bias, here with a fixed Gaussian noise level of $\sigma = 0.1$ DU. The RMSE error floor is due to the fixed non-zero value of $\sigma$. Again we observe that the RMSE with a uniform array is almost insensitive to the measurement bias and the corresponding estimation bias is zero. However, the RMSE for the non-uniform array increases linearly with, and is at a similar level to, the measurement bias. Similarly, estimation bias increases quickly with the measurement bias.

In order to gain a more intuitive insight into the bias effect, Figure 5 plots estimated source locations from 500 random realizations. Here, $K = 20$ sensors are uniformly circularly spaced. The source is at the origin, with radius $r = 1$ DU. Non-uniform bias was added as follows. Beginning with the first sensor (at $r = 1$, $\theta = 0$) and proceeding counter-clockwise, there are four groups of five sensors each. Each group has a common measurement bias, with groups 1 to 4 having biases of 0.4, 0.2, 0, and 0.05, respectively. All sensor measurements have the same noise standard deviation $\sigma = 0.2$. The resulting WLS location estimates show the bias effect, clustering in the third quadrant which is predominantly opposite sensor group 1 whose measurements had the most bias. Similarly, more points appear below the anti-diagonal line because group 2 in the second quadrant

has larger bias than group 4 in the fourth quadrant.

Next, in Figure 6, we consider five different sensor configurations, with $K = 10$ sensors again confined to the circle with unity radius. These are uniformly spaced, randomly placed, as well as the following three cases where the sensors are split into two groups of five sensors per group. In configuration 1, both groups are placed around 0 degrees as $(\pm 1, \pm 5, \pm 10, \pm 15, \pm 20)$ degrees. Configuration 2 centers groups around 0 and 90 degrees, given by $(-10, -5, 0, 5, 10, 80, 85, 90, 95, 100)$ degrees. Configuration 3 centers around 0 and 180, at $(-10, -5, 0, 5, 10, 170, 175, 180, 185, 190)$ degrees. Measurement biases are all zero in Figure 6(a), while $\mu = 0.1$ in Figure 6(b). As we expect, configuration 3 shows the best performance while configuration 1 shows the worst, as predicted in Section V. Configuration 2, random placement and fixed uniform placement all show similar intermediate performance. In particular, random placement and fixed uniform placement show almost indistinguishable performance. Compared with Figure 6(a), the non-zero bias for Figure 6(b) causes an error floor at $\sigma = 0$. Note that in configuration 3, the sensor angles differ from 0 and 180 degrees, giving rise to a non-zero location estimation bias as seen from (37).

Finally, we note that localization bias can arise due to the sensor-source geometry. Figure 7 plots estimates under four different configurations (similar to the above, but with $K = 10$ sensors for clarity; $\sigma = 0.1$). Here, all measurements are unbiased, so the resulting WLS localization bias is due solely to the sensor geometry.

## VII. Conclusions

We considered location estimation via weighted least squares, with possibly biased and noisy range measurements in a sensor network. An error analysis was performed for the WLS estimator based on a perturbation technique, yielding predictions of achievable performance. The small error analysis is shown to be accurate for a reasonable range of noise levels, and the error expressions can be used to accurately predict the impact of the biases, noise variance, and sensor placement. At low SNR, measurement bias becomes indistinguishable from the noise effect, whereas at high SNR it creates an RMSE noise floor. Topics of further interest include identifiability and theoretical bounds, as well as random modeling for the bias and associated estimators and bounds.

## References


[1] S. Pandey and P. Agrawal, "A survey on localization techniques for wireless networks," *Journal of the Chinese Institute of Engineers*, vol. 29, no. 7, pp. 1125-1148, 2006.

[2] L. Lazos and R. Poovendran, "SeRLoc: Secure range-independent localization for wireless sensor networks," *Proc. of the 2004 ACM Workshop on Wireless Security (WiSe04)*, pp. 21-30, 2004.

[3] T. He, C. Huang, B. M. Blum, J. A. Stankovic, and T. F. Abdelzaher, "Range-free localization schemes in large scale sensor networks," *Proc. of the Annual Intl. Conf. on Mobile Computing and Networking (MOBICOM03)*, pp. 81-95, 2003.

[4] A. Savvides, C.-C. Han, and M. Srivastava, "Dynamic fine-grained localization in ad-hoc networks of sensors," *ACM MOBICOM*, Rome, Italy, 2001.


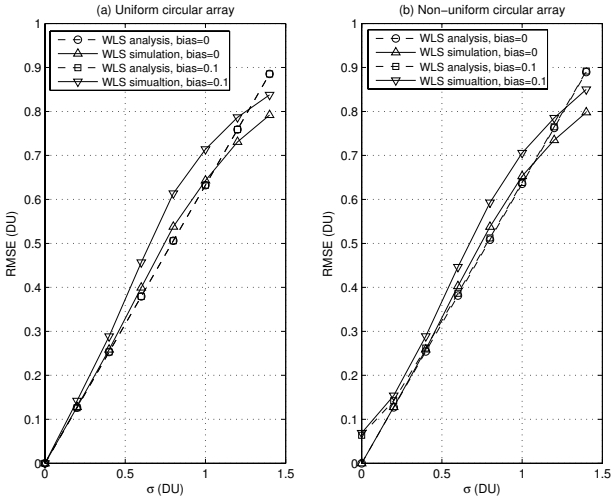


Fig. 1. RMSE of location estimation with uniform and non-uniform circular array for a large range of $\sigma$.

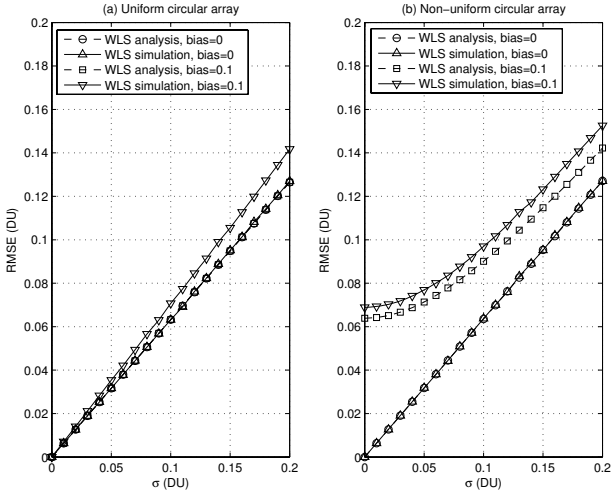


Fig. 2. RMSE of location estimation with uniform and non-uniform circular array for a small range of $\sigma$.

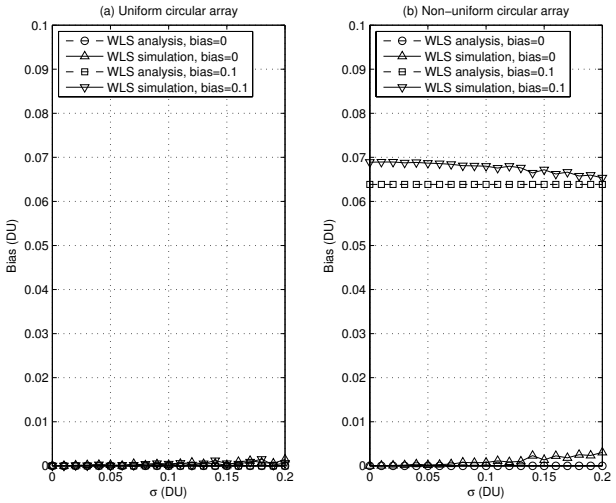


Fig. 3. Bias of location estimation with uniform and non-uniform circular array.

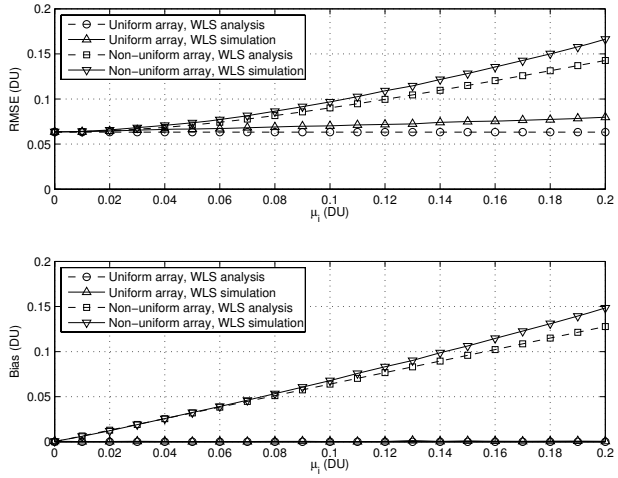


Fig. 4. Performance sensitivity to measurement bias, $\sigma = 0.1$.

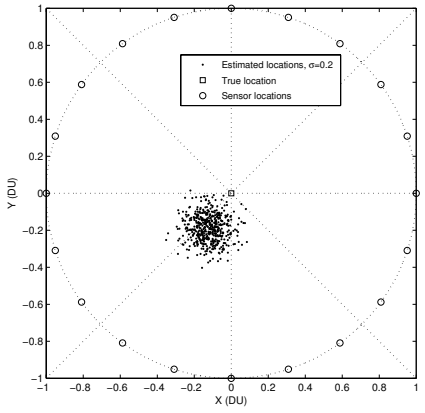


Fig. 5. Location estimates with non-uniform measurement bias, resulting in biased localization.

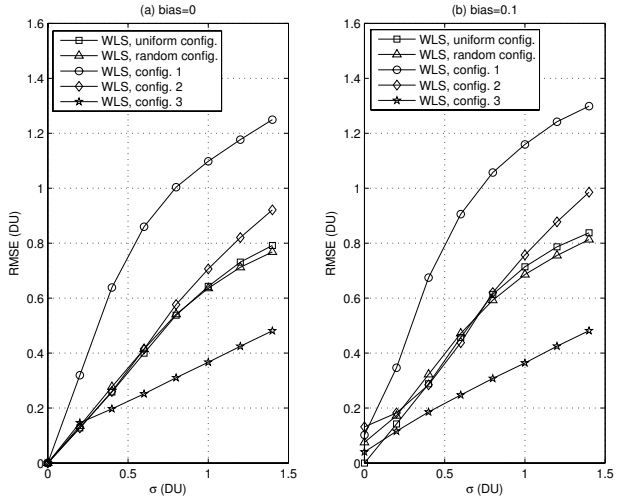


Fig. 6. Location estimation error for different sensor configurations, (a) without measurement bias, and (b) with measurement bias.

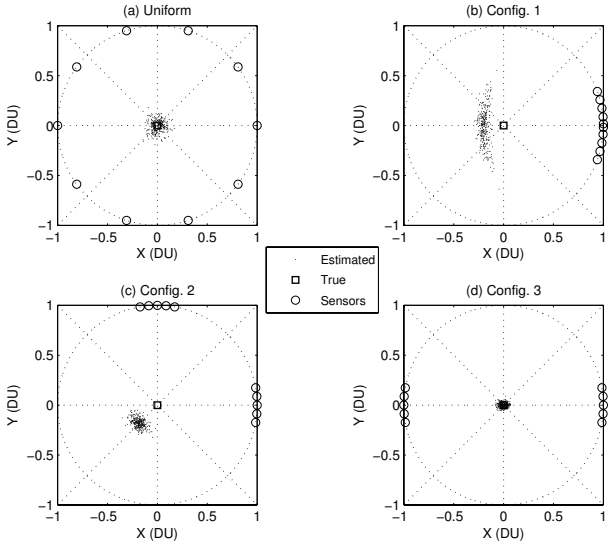


Fig. 7. Location estimates for different sensor configurations. All measurements are unbiased, so location bias is due solely to the sensor geometry ($\sigma = 0.1$, $K = 10$, source at the origin).


[5] S. Capkun, M. Hamdi, and J. Hubaux, "GPS-free positioning in mobile ad-hoc networks," *Proc. of the 34th Hawaii International Conference on System Sciences*, Jan. 2001.

[6] C. Savarese, J. M. Rabaey, and J. Beutel, "Location in distributed ad-hoc wireless sensor networks," *Proc. IEEE ICASSP*, pp. 2037-2040, May 2001.

[7] K. K. Chintalapudi, A. Dhariwal, R. Govindan, and G. Sukhatme, "Ad hoc localization using ranging and sectoring," *Proc. of IEEE INFOCOM,* vol. 4, pp. 2662-2672, 2004.

[8] A. J. Weiss and J. S. Picard, "Network localization with biased range measurements," *IEEE Trans. on Wireless Communications*, vol. 7, no. 1, pp. 298-304, January 2008.

[9] D. B. Jourdan, D. Dardart, and M. Z. Win, "Position error bound for UWB localization in dense cluttered environments," *IEEE Trans. on Aerospace and Electronic Systems*, vol. 44, no. 2, pp. 613-628, April 2008.

[10] Z. Xu and B. M. Sadler, "Time delay estimation bounds in convolutive random channels," *IEEE Journal of Selected Topics in Signal Processing: Special Issue on Performance Limits of Ultra-Wideband Systems*, vol. 1, no. 3, pp. 418-430, Oct. 2007.

[11] B. M. Sadler, N. Liu, and Z. Xu, "Ziv-Zakai bound on time delay estimation in unknown convolutive random channels," *Proc. of IEEE Sensor Array and Multichannel Signal Processing Workshop*, Darmstadt, Germany, July 21-23, 2008.

[12] R. J. Kozick, B. M. Sadler, "Bounds and algorithms for time delay estimation on parallel, flat fading channels," *Proc. Intl. Conf. on Acoustics, Speech, and Sig. Proc.,* (ICASSP'08), April 2008.

[13] N. Liu, Z. Xu, and B. M. Sadler, "Low complexity hyperbolic source localization with a linear sensor array," *IEEE Signal Processing Letters*, to appear.